

Metastable He_2^- and its autodetachment spectra: An accurate coupled-cluster study

Tadeusz Pluta and Rodney J. Bartlett

Quantum Theory Project, Department of Chemistry and Department of Physics, University of Florida, Gainesville, Florida 32611

Ludwik Adamowicz

Department of Chemistry, University of Arizona, Tucson, Arizona 85721

(Received 16 February 1989)

The unusual autodetachment spectrum of metastable He_2^- is studied theoretically, using high-level coupled-cluster methods and hybrid numerical and Slater orbital basis sets. By obtaining accurate curves for the repulsive wall of the ground $\text{He}_2(X^1\Sigma_g^+)$ state, the excited $\text{He}_2(a^3\Sigma_u^+)$ state, and the metastable $\text{He}_2(^4\Pi_g)$ state, we are able to provide an alternative explanation for the experimental observations, which had cast doubt on the veracity of the accepted curve for the repulsive part of the $\text{He}_2(X^1\Sigma_g^+)$ potential. We attribute the experimental peak at 15.78 ± 0.13 eV to transitions of vibrationally excited states ($\nu=2$ and higher) of He_2^- to the $\text{He}_2(X^1\Sigma_g^+)$ continuum, since the $\nu=0$ transition would have a value 1 eV less. An error of this size is considered to be far outside the error bars for highly accurate correlated *ab initio* calculations. The electron affinity of the $^4\Pi_g$ state of the anion (measured relative to $a^3\Sigma_u^+$) is computed to be 0.201 and 0.212 eV for different basis sets, compared to an experimental value of 0.175 ± 0.032 eV.

I. INTRODUCTION

The determination of the interaction energy of two helium atoms is a very old problem in quantum chemistry (see, e.g., Refs. 1 and 2). Although most attention has been paid to the Van der Waals region,¹⁻⁵ the repulsive part has also been investigated.⁶⁻⁸ Despite the small size of the He_2 system quantum calculations, especially around the Van der Waals minimum, are very challenging. This is mainly due to the necessity of using extremely large and carefully optimized basis sets while employing very accurate quantum-mechanical methods.⁸ Furthermore, the basis-set superposition error (BSSE) is known to play a critical role in this case, and for many basis sets will be larger than the Van der Waals depth itself.

Experimentally the repulsive region around 1 Å is also difficult to investigate, and as a result many empirical potentials differ substantially among themselves (e.g., Ref. 9). Bulk properties (like room-temperature viscosity) and various extrapolation techniques are used in developing these potentials. Recent Green's-function quantum Monte Carlo calculations performed by Ceperley and Partridge¹⁰ have provided a new Born-Oppenheimer potential between 0.5 and 1.5 Å. The authors claim that the statistical error at 1 bohr is about 0.2% (~ 0.05 eV) and drops to ~ 0.002 eV at $R = 1.75$ bohr. The Monte Carlo potential has been used in constructing a new empirical potential in the short-distance region.¹¹

A promising new technique to directly examine the repulsive $\text{He}_2(X^1\Sigma_g^+)$ potential curve in the vicinity of 1 Å is autodetachment spectroscopy.¹²⁻¹⁴ An advantage of this technique is the possibility of accurately measuring the energy of a transition from the vibrational level of the bound metastable state of the He_2^- anion into the repulsive continuum of $\text{He}_2(X^1\Sigma_g^+)$, which has been

termed "excimer"—autodetachment.¹³ By studying such transitions from the anion one can accurately predict the ground-state potential energy curve.

The metastable, relatively long-lived He_2^- anion assumed to exist in a $^4\Pi_g$ state was discovered recently¹⁴ and its autodetachment spectrum was recorded and analyzed subsequently.^{13,15} Some of the necessary information on the energies of the vibrational levels of He_2^- was provided by configuration-interaction (CI) calculations by Michels.^{16,17} Combining theoretical results for He_2^- and the observed spectrum, the potential curve deduced for $\text{He}_2(X^1\Sigma_g^+)$ is found to be similar in shape to the Monte Carlo curve but lies about ~ 1 eV above the latter. This discrepancy has attracted some attention and the recent paper of Bae *et al.*¹⁸ summarizes the situation and suggests (as we have¹⁹) that it might be necessary to consider transitions coming from the higher vibrational and/or rotational levels of the anion in order to fit the experimental spectrum. However, the inclusion of higher vibrational levels lead to additional difficulties connected with vibrational detachment into the excited triplet state of $\text{He}_2(a^3\Sigma_u^+)$. In particular, the energy of the $\nu=1$ state is quite close to that for the $a^3\Sigma_u^+$ state and detaches readily.

The CI results,^{16,17} though of good quality for the $\text{He}_2^-(^4\Pi_g)$ state, were not of sufficient quality to simultaneously describe the $\text{He}_2(X^1\Sigma_g^+)$ and $\text{He}_2(a^3\Sigma_u^+)$ states. Hence the computed $^4\Pi_g$ state was used together with the experimental curve for the $a^3\Sigma_u^+$ state and the quantum Monte Carlo curve for the $X^1\Sigma_g^+$ state to interpret the experimental results. Consequently, it is difficult to draw unambiguous conclusions about any potential inaccuracy of the quantum Monte Carlo curve. To rectify this inconsistency, all pertinent states need to be accurately computed at comparable levels of approximation.

In this paper we provide this information. We present the results of highly accurate coupled-cluster computations²⁰ of the repulsive part of the ground state of the He_2 ($X^1\Sigma_g^+$) potential curve. Second, in order to solve the puzzle of the He_2^- autodetachment, we have calculated the anionic potential energy curve for the $^4\Pi_g(1\sigma_g^2 1\sigma_u^1 2\sigma_g^1 1\pi_u^1)$ state of He_2^- . We have also obtained results for the “parent state” of He_2^- , namely, the excited $a^3\Sigma_u^+(1\sigma_g^2 1\sigma_u^1 2\sigma_g^1)$ state of He_2 . Using the calculated potential curves, the spectroscopic constants and vibrational levels of He_2^- and $\text{He}_2(a^3\Sigma_u^+)$ have been evaluated. A mechanism for the observed autodetachment transition consistent with our results is proposed.

This paper is organized as follows. Section II contains a brief description of the computational method used in this work. Section III presents results for the anion He_2^- , the excited triplet state and the repulsive ground state of He_2 . Our final conclusions are presented in Sec. IV.

II. DESCRIPTION OF THE METHOD

In previous work, we have shown that coupled-cluster theory with purely numerical orbitals can provide results that are among the most accurate ever obtained for diatomic molecules.^{21,22} Furthermore, we have demonstrated that a hybrid basis of numerical Hartree-Fock (NHF) and large numbers of Slater orbitals can be nearly as accurate,²³ but much more convenient for studies of potential energy curves.

Using coupled-cluster theory with a basis of numerical Hartree-Fock occupied orbitals and Slater functions, we have calculated the $X^1\Sigma_g^+$ and $a^3\Sigma_u^+$ potential curves for He_2 and the $^4\Pi_g$ curves for He_2^- and all transition energies can be obtained as differences between energies of the relevant states. For the open-shell systems, an unrestricted Hartree-Fock reference function is employed. Coupled-cluster single- and double-excitation CCSD (Ref. 24) and the CCSD+ T (CCSD) version²⁵ of the coupled-cluster method have been employed. In the latter the triple excitations are approximately included by using converged values of T_1 and T_2 coefficients obtained from CCSD by a single perturbative evaluation of the initial effects due to connected triple excitations T_3 . In general, CCSD+ T (CCSD) is close to the full CCSDT (Ref. 26) method and basis set limit full CI results for non-pathological cases. A full description of the coupled-cluster method and its various approximate versions can be found elsewhere.²⁰ Unlike most CI methods, the CC method is ideally suited to the calculation of weak intermolecular interactions, since at any given level of approximation, CCD, CCSD, or CCSD+ T (CCSD), it allows a molecule like He_2 in its ground state to separate smoothly into its noninteracting fragments. For the open shells, the appropriate unrestricted Hartree-Fock (UHF) function will also separate correctly, but the solution that separates correctly is one of several possible converged UHF solutions, depending upon which symmetries are broken.

The choice of basis set is of critical importance in any supermolecule-type computation of the interaction ener-

gy. Although the interaction energy could be obtained as a difference between two variational quantities, it is not a variational quantity itself. One practical consequence of this well-known fact is that a “better” basis set, i.e., one yielding a lower energy for a subsystems, can often lead to erroneous values of the interaction energy. In our present computations we have tried to achieve a reasonable compromise between basis-set accuracy while avoiding bias for particular states by generating a balanced set of correlating orbitals as a function of R . For the occupied orbitals, we have used numerical solutions of the Hartree-Fock problem in all our calculations.²⁷ These (NHF) orbitals are taken as a starting basis set, but instead of numerical correlating orbitals^{21,22} they are augmented by a set of Slater-type orbitals (STO). The mixed (or hybrid) numerical-analytical basis sets have been used for several small systems and proved to give satisfactory results for a variety of problems.²³

Reaching an optimum choice of analytical STO orbitals for general states is not easy, however. The traditional way of generating a basis set would be by optimization of the nonlinear parameters, but this is expensive and would require a different STO basis for each state, or even each choice of R . In the present case, we want to have the same basis set equally suited for all three very different states, to facilitate error cancellation in taking their differences. Hence we choose to use even-tempered construction of the basis set.²⁸ Even-tempered basis sets are easy to generate, and can be expected to be more flexible for different states, and thus better suited for our purpose of comparing the different states of neutral He_2 and its anion. In order to facilitate comparison with previous CI calculations by Michels¹⁶ we also perform a series of calculations using his original STO basis augmented by NHF solutions for the occupied orbitals. This basis set composed of ($4s2p1d$) orbitals on He or ($14\sigma6\pi2\delta$) in diatomic symmetry, which will be referred to as I, contains several diffuse exponent Slater functions chosen to describe the He_2^- anions. The exponents of our new STO basis (basis II), which can be denoted as ($5s6p3d1f$) (which gives $16\sigma20\pi8\delta2\phi$ in diatomic notation, see the explanation further in the text), cover approximately the range between basis I and the basis developed by Pouilly *et al.*²⁹ They are shown in Table I.

The usefulness of various STO bases has been tested by performing CCSD calculations (equivalent to the full CI in this case) on the helium atom. We calculate the ground-state energy of the $\text{He}(^1S)$ atom using the hybrid basis set I to be -2.877431 a.u. as compared to -2.873833 a.u. obtained by Michels.¹⁶ The improve-

TABLE I. Exponents of the basis set II. Only σ components of $2p$ orbitals with 1.6, 2.7, and 5.4 are kept. The basis can be denoted $16\sigma20\pi8\delta2\phi$.

Orbital	Exponents
1s	0.337, 0.623, 1.152, 2.129, 3.936
2p	0.208, 0.526, 0.950, 1.600, 2.700, 5.400
3d	0.413, 1.363, 4.500
4f	5.200

ment is due to CCSD being the full CI in the basis plus the addition of the NHF orbitals. However, both are rather far from the nonrelativistic *experimental-limit* value of -2.90320 a.u..³⁰ The absence of functions with large exponents which would primarily correlate the core electrons in this basis set is largely responsible for this failure. Basis II which augments basis I to correct this deficiency gives the He atom energy equal to -2.901582 a.u., or recovers 96% of the exact correlation energy. Retaining the small (diffuse) exponents of basis I in basis II should facilitate the correct description of the He_2^- anion. In a final effort to improve the analytic part of the hybrid basis we have added two $2s$ orbitals with the original Michels's exponent to our basis II. Again, as in the case of basis II in order to avoid linear dependencies caused by some redundancies among NHF and core orbitals, we have kept only the 3 most diffuse σ components from the p symmetry block, and all σ components of higher-angular-momentum shells have been rejected. The helium atom test energy is now only modestly improved to -2.901782 a.u. Since the size of basis II* ($20\sigma 20\pi 8\delta 2\phi$) makes the CCSD calculations more time consuming and slowly convergent, we use this basis set rather as a selective and useful check for the accuracy of the results of basis II rather than as another basis set. However, in the He_2^- case we have also computed several points on the potential energy curve with the more elaborate basis II*.

III. RESULTS

A. Short-range potential for $\text{He}_2(X^1\Sigma_g^+)$

The results for the He_2 repulsive ground-state potential for all our basis sets are given in Table II. In the same table the Monte Carlo values, those of Foreman *et al.*³¹ and the NHF results are shown for comparison. Foreman *et al.* obtained their ground-state He_2 repulsive potential curve from the measurements of the total scattering cross sections. The potential was assumed to be of the Born-Mayer form, and the experimental data were fitted to this curve. The Foreman curve is in excellent agreement with the NHF results, but somewhat poorer compared to the correlated and Monte Carlo results.

As seen from the table our calculated repulsive interaction energy for $\text{He}_2(X^1\Sigma_g^+)$ agrees very well with the

basis-set-independent quantum Monte Carlo results of Ceperley and Partridge.¹⁰ Furthermore, for the shape of the curve there is little difference between the CCSD+ T (CCSD) results for basis I and II, although there is a significant uniform shift due to basis I being less accurate for the He atom reference than basis II. There is also little difference between the CCSD basis II curve and that including triple excitations. The latter cannot contribute at all in the separated-atom limit, but their contribution for the four-electron problem is seen to be modest, anyway.

The analysis of photodetachment decay requires accurate values of the total energy range than the interaction energy. Taking into account the difference in the reference energy of He_2 at infinite internuclear separation ($E = -5.80640$ a.u.) one can see that the difference between the results of the CCSD+ T (CCSD) calculations (with basis II) and the Monte Carlo results is always smaller than ~ 0.1 eV. Basis I cannot produce as accurate results for the absolute energy due to the larger error in the reference energy [$\text{He}(^1S)$], but the shape of the curve is still accurate. It is worth noting that the CCSD+ T (CCSD) results using both basis sets at 1.04 \AA are in effective perfect agreement with the experimental value of 3.4 ± 0.1 eV.³² It is also interesting to observe that both the experimental Foreman potential and NHF curve are nearly identical though systematically shifted about 0.1 – 0.2 eV higher than our results.

Previous *ab initio* calculations^{6,7} yield energies for the ground-state potential energy curve differing by as much as 0.74 eV at 0.9 \AA and 0.32 eV at 1.3 \AA . The present results are in sharp disagreement with Matsumoto *et al.*⁶ natural-orbital–configuration–interaction (NO-CI) calculations. The CI curve by Philipson⁷ is more acceptable, being in error by ~ 0.1 eV at 1.0 \AA and 0.15 eV at 1.1 \AA . However, one can notice that the shape of Philipson's curve is also different. From the above the ground-state potential, at least in the non-Van der Waals region, seems to be correctly established and we do not think improved calculations will change this situation significantly.

B. $\text{He}_2^-(a^4\Pi_g)$

Bae and co-workers^{14,18} suggested that the electronic state of the newly discovered anion is either the $^4\Pi_g(1\sigma_g^2 1\sigma_u^2 2\sigma_g^1 1\pi_u^1)$ or $^4\Sigma_g^+(1\sigma_g^2 1\sigma_u^2 2\sigma_g^1 2\sigma_u^1)$ state. CI

TABLE II. Coupled-cluster interaction energies for the $(X^1\Sigma_g^+)\text{He}_2$ system (energies in eV, distances in \AA).

R	Basis I		Basis II		Basis II*		Monte Carlo	NHF	Foreman <i>et al.</i>
	CCSD+ T (CCSD)	CCSD	CCSD+ T (CCSD)	CCSD+ T (CCSD)	CCSD+ T (CCSD)				
0.7	12.97	12.97	12.97				12.98	13.35	13.56
0.8	8.80	8.80	8.81				8.78	9.10	9.13
0.9	5.92	5.93	5.94				5.89	6.17	6.15
1.0	3.96	3.97	3.98		3.98		3.94	4.15	4.15
1.04	3.37	3.38	3.39				3.34	3.54	3.54
1.1	2.64	2.65	2.61		2.65		2.61	2.78	2.79
1.12	2.43	2.45	2.44		2.45		2.41	2.56	2.58
1.3	1.15	1.16	1.16				1.13	1.23	1.27

TABLE III. Potential energy curve for the ${}^4\Pi_g$ state of He_2^- (distances are in Å, energies in a.u. or cm^{-1}).

R	Basis I		Basis II		Basis II*	Basis II ^a
	CCSD T (CCSD)	CCSD	CCSD+ T (CCSD)	CCSD+ T (CCSD)	CCSD+ T (CCSD)	CCSD+ T (CCSD)
0.7	-5.010 854	-5.038 147	-5.038 753	-5.039 515	167 769	
0.8	-5.081 485	-5.107 452	-5.108 065	-5.108 627	152 557	
0.9	-5.116 703	-5.141 178	-5.141 824	-5.142 307	145 148	
1.0	-5.130 270	-5.153 715	-5.154 421	-5.154 863	142 383	
1.1	-5.131 125	-5.154 047	-5.154 843	-5.155 254	142 290	
1.2	-5.125 291	-5.147 764	-5.148 682	-5.149 451	143 642	
1.3	-5.115 918	-5.138 317	-5.139 397	-5.139 791	145 680	
1.5	-5.095 129	-5.117 347	-5.118 397		150 178	
1.75	-5.074 063	-5.095 357	-5.097 870		154 795	
2.0	-5.060 958	-5.080 797	-5.084 732		157 678	
2.5	-5.052 037	-5.068 182	-5.075 825		159 633	
E_{\min}	-5.131 962		-5.155 756			
R_e	1.056		1.053			

^aThe energy in cm^{-1} is related to $\text{He}(^1S) + \text{He}(^1S) = 0$ as a reference energy.

computations by Michels^{16,17} showed that the ${}^4\Pi_g$ state is stable relative to the decay to $\text{He}_2(a^3\Sigma_u^+) + e^-$. The possibility of the (${}^4\Sigma_g^+$) state being responsible for the auto-detachment was rejected by Michels¹⁷ since this state appears to correspond to a resonance state. This conclusion was justified by applying the stabilization (i.e., modified nuclear charge Hamiltonian) method.³³ Our NHF analysis presented elsewhere²⁷ also clearly demonstrates this fact and the extreme diffuseness of the outer $2\sigma_u$ orbital. At R equal to 1.1 Å the orbital energy of $2\sigma_u$ approaches zero and the extra electron leaves the ion.²⁷

In our present study we concentrate on the (${}^4\Pi_g$) state. Table III contains the energy curve for this state, while Fig. 1 shows the relative orientation of all the relevant states. The last column displays the relative energy of the anion with respect to the energy of the two noninteracting $\text{He}(^1S)$ atoms as a reference. The values given in this column should make direct comparison with CI results easy.

Since the basis set of Michels (i.e., I) was not adequate to describe the $a^3\Sigma_u^+$ state of He_2 , the author adjusted his

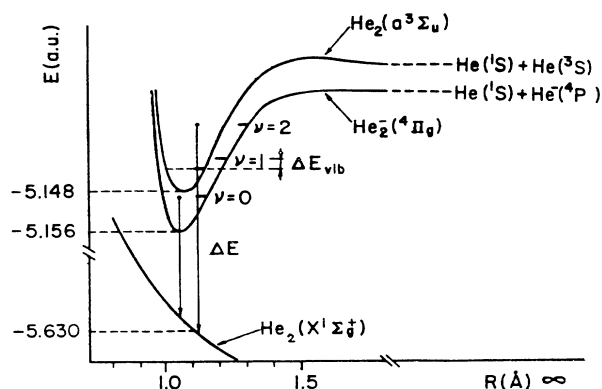


FIG. 1. Total energy curves for He_2 and He_2^- .

calculated CI curve with the experimentally known Rydberg-Klein-Rees (RKR) potential for that state of He_2 . This procedure enabled him to make more meaningful comparisons.

As can be seen from Table III the potential curve for He_2^- is rather sensitive to the quality of basis set used. A change from basis I to the more extended basis II causes a downward shift in the energy minimum of ~ 0.65 eV. The bond length is not altered much when the basis set is improved, however. The basis II* still improves the results but now the change is typically of the order of 0.01–0.02 eV, well below the tolerance we require for most of our interpretations. The spectroscopic constants of He_2^- as predicted by our calculations with basis I are close to those of Michels, while once the basis set is improved the gap between the results widens.

Although, the long-range region is not pertinent to the explanation of the autodetachment experiment, a short comment might be pertinent. The He_2^- ion dissociates into $\text{He}(^1S)$ and $\text{He}^-(^4P)$. The atomic $\text{He}^-(1s2s2p)$ cannot be correctly described at the Hartree-Fock level, since 4P He^- is unbound at that level. The energy of the $2p$ orbital approaches zero causing the numerical HF solution to become the solution for (3S)He. Hence, we cannot employ an NHF reference for CC calculations for the asymptotic region of the curve. For intermediate values of R the necessity of breaking the $1\sigma_g$ double-occupancy condition to achieve correct separation either requires a multireference description as discussed by Michels¹⁶ or a carefully determined unrestricted Hartree-Fock solution. We use the latter, but the impending multireference character causes the perturbative triple excitation contribution to the CCSD method, $T(\text{CCSD})$, to behave erratically, as seen in Table III, where it increases rapidly for larger R . This is indicative of the failure of the perturbation analysis involved in the $T(\text{CCSD})$ evaluation when the orbital energies causes an impending denominator singularity. We can avoid using multireference many-body perturbation theory (MBPT)

TABLE IV. Potential energy curve for the $^3\Sigma_u^+$ state of He₂ (distances are in Å, energies in a.u. or cm⁻¹).

<i>R</i>	Basis I	Basis II	Basis II*	Basis II ^a
	CCSD + <i>T</i> (CCSD)	CCSD + <i>T</i> (CCSD)	CCSD + <i>T</i> (CCSD)	
0.7	-5.006 448	-5.034 608		168 679
0.8	-5.076 383	-5.102 553		153 767
0.9	-5.110 612	-5.135 260		146 588
1.0	-5.123 335	-5.147 075	-5.147 217	143 995
1.05	-5.124 458	-5.148 095	-5.148 212	143 771
1.1	-5.123 682	-5.146 942	-5.147 040	144 024
1.2	-5.117 371	-5.140 447		145 450
1.3	-5.107 848	-5.131 018		147 519
1.5	-5.087 497	-5.110 731		151 972
1.75	-5.067 949	-5.090 733		156 361
2.0	-5.056 705	-5.079 055		158 924
2.5	-5.049 784	-5.072 373		160 390
<i>E</i> _{min}	-5.124 645	-5.148 102		
<i>R</i> _{<i>e</i>}	1.050	1.045		

^aSee footnote of Table III.

calculations by including triples iteratively as in CCSDT (Ref. 26) or CCSDT-1 (Ref. 25). However, since all interpretations pertain to curves in the vicinity of ~ 1 Å, our results for that region should not be affected by the potentially erroneous behavior in the asymptotic region.

C. He₂($a^3\Sigma_u^+$)

In the case of the $a^3\Sigma_u^+$ state of He₂ the situation is clearer. Changing from basis I to II results in an overall improvement with the experimental values for the spectroscopic constants. The curves calculated with basis II and II* are very close to that reported recently by Konowalow and Lengsfeld³⁴ who used the multiconfiguration SCF (MCSCF) method and a carefully generated STO basis set. The spectroscopic constants agree very well with the experimental values^{35,36} and

some of those previously evaluated theoretically. *T*₀₀ calculated with basis II is 144 788 cm⁻¹ at the CCSD level, in almost perfect agreement with the experimental value of 144 935 cm⁻¹.³⁵ Approximate inclusion of the triple excitations gives 143 746 cm⁻¹. The results for the $a^3\Sigma_u^+$ state are displayed in Table IV and the spectroscopic constants are summarized in Table V.

As in the case of the $^4\Pi_g$ state at large *R* one has to use the UHF-NHF method carefully to correctly describe the dissociation process of the $a^3\Sigma_u^+$ state. But once again, as justified by comparison of our results with the experimental data, there are no residual problems in the important region around 1 Å.

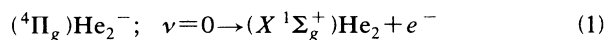
D. Interpretation of the photodetachment spectrum

Considering Fig. 1, the interpretation of the observed autodetachment spectrum of the metastable He₂⁻ anion

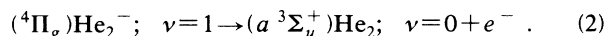
TABLE V. Spectroscopic constants for He₂ and He₂⁻

State, method	ω_e (cm ⁻¹)	$\omega_e x_e$ (cm ⁻¹)	α_e (cm ⁻¹)	<i>B</i> _{<i>e</i>} (Å)	<i>R</i> _{<i>e</i>} (Å)
$a^3\Sigma_u^+$ state					
Experiment (Ref. 35)	1808.6	37.1	0.2281	7.704	1.046
CCSD + <i>T</i> (CCSD), basis II	1806.9	37.6	0.2332	7.700	1.045
CCSD, basis II	1816.2	37.0	0.2300	7.715	1.045
CCSD + <i>T</i> (CCSD), basis I	1808.8	33.0	0.2172	7.618	1.050
MCSCF (Ref. 34)	1814.1				1.046
MCSCF (Ref. 36)	1794.5	36.4	0.2291	7.634	1.050
$^4\Pi_g$ state					
Experiment (Ref. 15)	1500				
CCSD + <i>T</i> (CCSD), basis II	1797.0	37.5	0.2279	7.611	1.054
CCSD, basis II	1805.7	36.8	0.2253	7.626	1.050
CCSD + <i>T</i> (CCSD), basis I	1801.3	33.9	0.2067	7.520	1.056
CI (Ref. 17)	1761.8	30.1	0.1910	7.448	1.064
CI (Ref. 16)	1783.0	42.7	0.2502	7.600	1.053

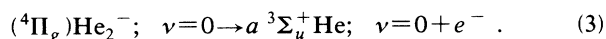
as offered by Kvale *et al.*¹⁵ and Bae *et al.*¹⁸ consists of three assignments. The energy peak with a maximum at 15.78 ± 0.13 eV (or 15.70 ± 0.15 eV¹⁸) is explained as the electronic transition



and the weak peak of 11.5 ± 2.6 meV is assigned to originate from the vibrational detachment,



The third observation is the electron affinity obtained from



The calculated energies of these transitions using both basis sets are summarized in Table VI. The poorer basis, I, gives rather erroneous values for electron detachment into the repulsive ground-state continuum of 14.1 eV. When basis II is employed the energy of the transition to the repulsive ground-state is 14.8 eV, which is still about 1 eV less than the assigned experimental value, but should be sufficiently accurate to conclude that the remaining 1 eV discrepancy with experiment is too great to be ascribed to additional inaccuracies in the computations.

In basis I the vibrational photodetachment energy is predicted to be 15 meV in good agreement with 11.5 ± 2.6 meV. However, in basis II, it is rather poorly predicted to be 3 meV; but considering the very small value, this discrepancy is evidently the result of destroying the delicate and fortuitous balance of errors in the description of He_2^- and the excited triplet state of He_2 which apparently exists for basis I.

The discrepancy for transitions (1), however, calls for a different explanation. When a better basis set is used to describe the electronic structure of He_2^- the energy of the ${}^4\Pi_g$ state will almost certainly be lowered. Yet since no major changes of the energy curve for the ground state of He_2 are expected at short distances, the poor agreement of the transition energy with the observed peak would be expected to deteriorate further.

The most plausible explanation of the observed process is to allow transitions from higher vibrational levels. As can be seen from Table II, the transition from the $\nu=2$ level releases energy equal to 15.2 and 15.7 eV for basis I and II, respectively, the latter in almost perfect agreement with the experimental value. Populating higher vibrational levels only adds to the electronic energy transitions two small vibrational quanta, but by virtue of increasing the effective R_e of He_2^- to ~ 1.12 Å adds about an 1 eV to the vertical transition to the repulsive He_2 ground state. Furthermore, the $\nu=1$ level of He_2^- autoionizes to the $\text{He}_2(a^3\Sigma_u^+)$ state depopulating that level, requiring significant residual population in *higher* vibrational levels to account for the observed energy transition. This interpretation¹⁹ is supported by the recent analysis of Bae *et al.*¹⁸ who constructed several models of higher vibrational transitions to fit the experimental autodetachment energy and the existing quantum Monte Carlo curve for He_2 .

TABLE VI. Calculated CCSD + T(CCSD) photodetachment energies for He_2 (eV).

Vibrational level	Basis I	Basis II
Photodetachment into repulsive ground state $({}^4\Pi_g)\text{He}_2^- \rightarrow (X^1\Sigma_g^+)\text{He}_2 + e^-$		
$\nu=0$	14.1	14.7
$\nu=2$	15.2	15.7
Photodetachment into the $a^3\Sigma_u^+$ state of He_2 $({}^4\Pi_g)\text{He}_2^-; \nu=1 \rightarrow (a^3\Sigma_u^+)\text{He}_2; \nu=0 + e^-$		
	0.015	0.003
Electron affinity $a^3\Sigma_u^+\text{He}_2; \nu=0 \rightarrow {}^4\Pi_g\text{He}_2^-; \nu=0$		
	0.201	0.212

The electron affinity of the He_2^- anion ($\nu=0$) as in transition (3) is 0.201 and 0.212 eV for basis I and II, respectively. The triple excitation contribution for basis II is negligible, with the CCSD result being 0.204 eV. Our results are close to the experimental result 0.175 ± 0.032 eV.¹³ In addition the present results are in good agreement with the CI results of Michels¹⁶ (0.233 eV) and (0.182 eV).¹⁷ However, the latter depended upon a knowledge of the experimental curves for the $a^3\Sigma_u^+$ state.

The competition between autodetachment into the continuum and vibrational autodetachment is not yet understood. The present results point to the necessity of including at least transitions from the second vibrational level of the anion to explain the observed results in the ${}^4\Pi_g$ state. It would seem that the population in this state is selective, with the $\nu=1$ state being depopulated. Alternatively, the peak at 15.8 eV would have to correspond to a transition from an entirely different electronic state of He_2^- .

Other potential errors in the calculation which might affect these conclusions would be an unusual BSSE correlation error that would artificially lower the $X^1\Sigma_g^+$ curve. However, recent calculations of Van Lenthe *et al.*,¹⁸ who used a large Gaussian basis set (up to 131 functions) and the multireference CI (MR-CI) technique and employed the full counterpoise corrections to eliminate BSSE, are in good agreement with both our potential and the quantum Monte Carlo curve. Furthermore, only the total energies of He_2^- and $\text{He}_2(a^3\Sigma_u^+)$ states which are well-bound and could only be slightly affected (< 0.05 eV) if any by BSSE, plus the energy of the $X^1\Sigma_g^+$ curve are used to analyze the photodetachment experiment, no BSSE can significantly affect our conclusions.

ACKNOWLEDGMENTS

This paper has benefited from several useful conversations with Dr. Robert Compton. This work has been supported by the U.S. Air Force Office of Scientific Research under Contract No. AFOSR-89-0207.

- ¹J. H. Van Lenthe, J. G. C. M. Van Duijneveldt-van de Rijdt, and F. B. Van Duijneveldt, *Adv. Chem. Phys.* **57**, 521 (1987).
- ²G. Chalasinski and M. Gutowski, *Chem. Rev.* **88**, 943 (1988).
- ³B. Liu and A. D. McLean, *J. Chem. Phys.* **72**, 3418 (1980).
- ⁴P. G. Burton, *J. Chem. Phys.* **70**, 3112 (1979).
- ⁵M. Gutowski, J. Verbeek, J. H. Van Lenthe, and G. Chalasinski, *Chem. Phys.* **111**, 271 (1987).
- ⁶G. H. Matsumoto, C. F. Bender, and E. R. Davidson, *J. Chem. Phys.* **46**, 402 (1967).
- ⁷P. E. Philipson, *Phys. Rev.* **125**, 1980 (1962).
- ⁸J. H. Van Lenthe, R. J. Vos, J. G. C. M. Van Duijneveldt-Van de Rijdt and F. B. Van Duijneveldt, *Chem. Phys. Lett.* **143**, 435 (1988).
- ⁹G. Scoles, *Ann. Rev. Phys. Chem.* **31**, 81 (1980).
- ¹⁰D. M. Ceperley and H. Patridge, *J. Chem. Phys.* **84**, 820 (1986).
- ¹¹R. A. Aziz, F. R. W. McCourt, and C. C. K. Wong, *Mol. Phys.* **61**, 1487 (1987).
- ¹²P. S. Drzaic, J. Marks, and J. I. Brauman, in *Gas Phase Ion Chemistry*, edited by M. T. Bowers (Academic, New York, 1984).
- ¹³T. J. Kvale, R. N. Compton, G. D. Alton, J. S. Thompson, and D. J. Pegg, *Phys. Rev. Lett.* **56**, 592 (1986).
- ¹⁴Y. K. Bae, M. J. Coggiola, and J. R. Peterson, *Phys. Rev. Lett.* **52**, 747 (1984).
- ¹⁵T. J. Kvale, R. N. Compton, G. D. Alton, J. S. Thompson, and D. J. Pegg (unpublished).
- ¹⁶H. H. Michels, *Phys. Rev. Lett.* **52**, 1413 (1984).
- ¹⁷H. H. Michels, *Chem. Phys. Lett.* **126**, 537 (1986).
- ¹⁸Y. K. Bae, J. R. Peterson, H. H. Michels, and R. H. Hobbs, *Phys. Rev. A* **37**, 2778 (1988).
- ¹⁹T. Pluta, R. J. Bartlett, and L. Adamowicz (unpublished).
- ²⁰R. J. Bartlett, *J. Phys. Chem.* **93**, 1697 (1989); *Ann. Rev. Phys. Chem.* **32**, 359 (1981); R. J. Bartlett, C. E. Dykstra, and J. Paldus, in *Advanced Theories and Computational Approaches to the Electronic Structure of Molecules*, edited by C. E. Dykstra (Reidel, Dordrecht, 1984), pp. 127–159.
- ²¹L. Adamowicz and R. J. Bartlett, *J. Chem. Phys.* **83**, 6760 (1985); L. Adamowicz, R. J. Bartlett, and E. A. McCullough, *Phys. Rev. Lett.* **54**, 426 (1985).
- ²²L. Adamowicz and R. J. Bartlett, in *Applied Quantum Chemistry*, edited by V. H. Smith, H. F. Schaefer III, and K. Morokuma (Reidel, Dordrecht, 1986), p. 111; L. Adamowicz and R. J. Bartlett, *Int. H. Quantum Chem.* **31**, 183 (1987).
- ²³L. Adamowicz and R. J. Bartlett, *Chem. Phys. Lett.* **129**, 159 (1986); *J. Chem. Phys.* **88**, 313 (1988).
- ²⁴G. D. Purvis III and R. J. Bartlett, *J. Chem. Phys.* **76**, 1910 (1982).
- ²⁵M. Urban, J. Noga, S. J. Cole, and R. J. Bartlett, *J. Chem. Phys.* **83**, 4041 (1985).
- ²⁶J. Noga and R. J. Bartlett, *J. Chem. Phys.* **86**, 7041 (1987); **89**, 3401(E) (1988).
- ²⁷T. Pluta, R. J. Bartlett, and L. Adamowicz, *Int. J. Quantum Chem. Symp.* **22**, 225 (1988).
- ²⁸K. Ruedenberg, R. C. Raffanetti and R. D. Bardo, in *Energy Structure and Reactivity*, Proceedings of the 1972 Boulder Conference on Theoretical Chemistry (Wiley, New York, 1973), p. 164.
- ²⁹B. Pouilly, B. H. Lengsfeld, and D. R. Yarkony, *J. Chem. Phys.* **80**, 5089 (1984).
- ³⁰A. Weiss, *Phys. Rev.* **122**, 1826 (1961).
- ³¹P. B. Foreman, P. K. Rol, and K. P. Coffin, *J. Chem. Phys.* **61**, 1658 (1974).
- ³²H. H. Michels, R. H. Hobbs, and J. R. Peterson, *Chem. Phys. Lett.* **134**, 571 (1987).
- ³³B. Nestmann and S. D. Peyerimhoff, *J. Phys. B* **18**, 615 (1985).
- ³⁴D. D. Konowalow and B. H. Lengsfeld, *J. Chem. Phys.* **87**, 4000 (1987).
- ³⁵K. P. Huber and G. Herzberg, in *Molecular Spectra and Molecular Structure* (Van Nostrand Reinhold, New York, 1977), Vol. 4.
- ³⁶K. K. Sunil, J. Lin, H. Siddiqui, P. E. Siska, K. D. Jordan, and R. Shepard, *J. Chem. Phys.* **78**, 6190 (1983).